

Binding sites on the outside of metallo-supramolecular architectures; engineering coordination polymers from discrete architectures†

Mirela Pascu, Floriana Tuna, Edyta Kolodziejczyk, Gabriel I. Pascu, Guy Clarkson and Michael J. Hannon*

Centre for Supramolecular and Macromolecular Chemistry, Department of Chemistry, University of Warwick, Gibbet Hill Road, Coventry, UK CV4 7AL.
E-mail: M.J.Hannon@warwick.ac.uk

Received 11th March 2004, Accepted 2nd April 2004

First published as an Advance Article on the web 21st April 2004

Aggregation of metallo-supramolecular architectures through additional coordination is explored by introducing metal-binding units onto the outside of the supramolecular architectures. This is achieved within the framework of our imine-based approach to supramolecular architecture, by replacing the pyridylimine units with pyrazylketimine units. An advantage of the design is that it retains the ease-of-synthesis which characterises our imine-based approach. Silver(I) complexes of three pyrazylketimine ligand systems are described. The complexes demonstrate that introducing pyrazine donor units does indeed allow higher-order assembly of the distinct supramolecular architectures into engineered coordination polymers. Two distinct types of aggregation are observed. In the first, the donors on the outside of one architecture bind to the metals of another to link the units into a polymeric array. In the second type, the donors on the outside of the architectures bind to separate metal centres which are themselves not part of the architectures, and these separate metal centres link the units to form the macromolecular array. The weaker donor nature of the pyrazine nitrogens (compared to pyridine) also introduces an additional element into the design; higher coordination numbers are favoured and this can lead to arrays with higher connectivity than those observed in the discrete pyridylimine architectures.

Introduction

The design of complex molecular architectures using supramolecular methodology is a topic of much current interest and has afforded a variety of different nanoscale structures with dimensions greater than those associated with covalent synthetic approaches.¹ The increase in size and in architectural complexity are clear benefits of the approach, but nevertheless the approach does rely, at least in part, on covalent synthesis to construct the molecular building blocks which are then assembled through the supramolecular interactions. Simplifying (or minimising) the covalent aspects of the synthesis is central to the ability to build up large supramolecular species rapidly. In this context we have championed the use of pyridylimine ligands to assemble complex metallo-supramolecular arrays in one-pot reactions (either with or without solvent) from commercial aldehydes, amines and metal salts.^{2–10} Freed from extensive covalent synthetic procedures (our covalent synthesis is a simple condensation reaction), we have been able to systematically explore the design features of such arrays, developing routes to encode the precise microstructure of the supramolecular architectures,³ and importantly to explore the properties of the supramolecular arrays.⁴

While the covalent synthetic steps may be minimised, they nevertheless limit the dimensions of the building blocks and thus of the supramolecular architecture constructed. To move to larger arrays, one approach that we^{5–6,11,12} and others¹³ are developing is the use of multiple recognition events in concert. Thus in an initial supramolecular event the covalent building blocks are assembled into a distinct supramolecular architecture, and then, in a second supramolecular event, this supramolecular architecture is assembled into a higher-order array. We have recently described examples where π – π inter-

actions⁵ or hydrogen-bond interactions⁶ are used to assemble pyridylimine metallo-supramolecular architectures into higher-order structures. Herein we extend this approach by exploring the use of metal–ligand interactions to aggregate such architectures.¹⁴

Molecular design

To investigate metal-based aggregation, our approach is to incorporate additional donor groups into the covalent ligand framework such that when the architecture is assembled, these additional donors point out of the architecture and are available to link the distinct architectures into larger arrays. To achieve this we chose to replace the pyridine of our pyridylimine ligands with a pyrazine. In effect, this adds an additional nitrogen opposite the pyridylimine binding site and pointing out of the architecture. Our design approach is illustrated schematically in Fig. 1. The advantage of adding the additional functionality at the pyridylimine unit, rather than within a spacer group, is that it allows us to explore the effect of the

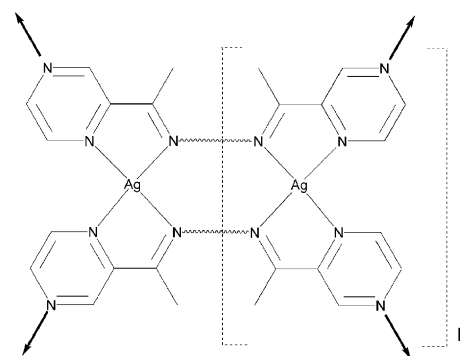


Fig. 1 Schematic representation illustrating the design approach investigated herein in which pyrazylketimines are used in place of pyridylimines to afford additional aggregation sites on the exterior of metallo-supramolecular units.

† Electronic supplementary information (ESI) available: Fig. S1: View showing the herringbone style packing of the π -stacked columns in the structure of ligand L_n . See <http://www.rsc.org/suppdata/dt/b4/b403749a/>

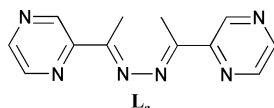
aggregation unit within a range of different ligand systems that give rise to various different architectures. Three such ligand systems are investigated herein.

Previously, in a polypyridyl ligand system which supports metallo-supramolecular box formation, we have attached thioether groups to the back of a pyridine ring and demonstrated that these groups can then be used to aggregate the box units through metal coordination.¹¹ The aggregation site in these pyrazylketimine systems will be different since the aggregation site is now contained within the same aromatic ring as one of the donors which assembles the architecture. Consequently the aggregation site has the potential to influence, and/or be influenced by, the architecture-forming site.

Pyrazines themselves are well known dinucleating ligands and, as with many dinucleating N-heterocyclic ligands, have attracted much attention from crystal engineers. Of particular relevance to the work described herein, the coordination of pyrazine to silver(I) gives a wide range of different possible structures in which the silver exhibits coordination numbers in the range two to six.^{15–17}

Results and discussion

Ligand L_a and its silver(I) complexes



To initiate our studies, we explored the system in which the two pyrazylketimine units are directly linked through the imino nitrogens without a spacer between the binding sites (L_a). We have made a number of detailed explorations of the corresponding pyridylimine ligands bearing different substituents at the imino carbon.^{7–9} We found that when these ligands bound d^{10} monocations a library of different solution architectures was possible, including planar dimers, double-helices, triple-helices and circular helicates of varying nuclearity. The presence of substituents at the imino carbon enforces ligand twisting and thus adoption of helical architectures. In the dimeric double-helical complexes, the silver(I) centres appear dissatisfied with the coordination environment offered by the ligand and were observed to form additional long interactions to anions or solvent molecules (Fig. 2).^{8,9} Indeed, the constraints of the ligand lead to significant distortion from tetrahedral coordination, creating vacant sites for such interaction. Such architectures were thus attractive since the additional pyrazine nitrogens from other units might fulfil this additional coordination role in place of the anions/solvent. This made the L_a ligand system the starting point for our investigations.

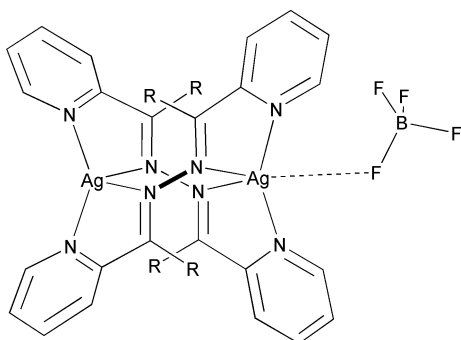


Fig. 2 Schematic representation of the interaction of an anion with the double-helical cation in the analogous pyridylimine system. Solvent molecules are also observed to interact in a similar fashion.

The ligand L_a is readily prepared by condensation of two equivalents of pyrazinemethylketone with one equivalent of hydrazine. Crystals of the ligand were obtained from the reac-

tion mixture on standing and X-ray crystallography confirms the expected ligand structure (Fig. 3). In the solid-state structure, the ligand is essentially planar and is π -stacked into columns, such that the imine unit of one ligand lies above the pyrazine ring of another. The ligand adopts a *trans* configuration about the central N–N bond and the pyrazine N1 nitrogen is similarly *trans* to the imino nitrogen as would be anticipated (minimising proton–proton interactions while maximising conjugation) and as observed in pyridylimine systems.^{10,18} The π -stacked columns are packed together in a herringbone fashion (see Fig. S1, ESI†).

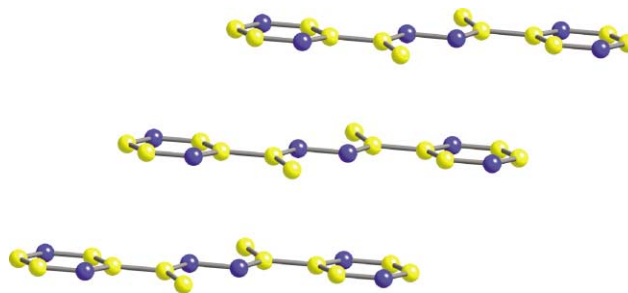


Fig. 3 Crystal and molecular structure of the ligand L_a illustrating the π -stacked columns of ligands. Hydrogens are omitted for clarity.

The ligand L_a was reacted with one equivalent of silver(I) hexafluorophosphate to afford a white solid, crystals of which were obtained from acetonitrile by slow diffusion of tetrahydrofuran. The crystal structure reveals a complex of 1 : 1 stoichiometry containing dinuclear double-helical units (Fig. 4).

These double-helical units comprise two silver(I) centres each attached to two didentate pyrazylketimine binding units from two different ligands. The ligands wrap around the metal–metal axis giving rise to the double-helical architecture on the outside of which are located the monodentate pyrazine nitrogens. These double-helical structural units are analogous to those that we have characterised for the corresponding pyridylimine ligand systems.^{7–9} However, the additional pyrazine nitrogens do have the desired aggregation effect and link these double-helical units together by coordinating to the silver(I) centres of adjacent units. There are two such interactions to each helix, both to the same metal centre. The other metal centre interacts with an acetonitrile solvent molecule. The interactions are long ($\text{Ag} \cdots \text{N}_{\text{pz}} 3.32 \text{ \AA}$; $\text{Ag} \cdots \text{N}_{\text{MeCN}} 3.46 \text{ \AA}$) as observed previously for solvent and anion interactions in the corresponding pyridylimine systems.^{7–9,19} The silver(I) centres within the cations are separated by 4.42 \AA . The twisting of the ligand strands (which is essential for helicate formation) takes place primarily about the N–N bond between the binding units (torsion angle 98°), and the pyrazylketimine units are close to planar (dihedral angles in the range $10\text{--}15^\circ$). The $\text{Ag}\text{--}\text{N}_{\text{pz}}$ and $\text{Ag}\text{--}\text{N}_{\text{im}}$ distances within the helices are similar to those observed in the pyridylimine systems, with the bonds to the imino nitrogens slightly longer than those to the pyrazines due to the constraints of the structure.

The interactions between the double-helical units link them into a two-dimensional network. These two-dimensional planes are stacked together creating square channels in which the hexafluorophosphate anions reside (Fig. 5) making short contacts to the pyrazine and methyl protons and the acetonitrile.

The complex has poor solubility, having some solubility in acetonitrile and nitromethane, but being only very poorly soluble in solvents such as acetone and dichloromethane. This is in contrast with the corresponding discrete pyridylimine complexes and is consistent with the solid-state polymeric structure described herein. We were able to obtain weak ^1H NMR spectra in acetonitrile and nitromethane solutions. At room temperature a single set of peaks were observed in each case. As we have previously shown this is unrevealing, being consistent

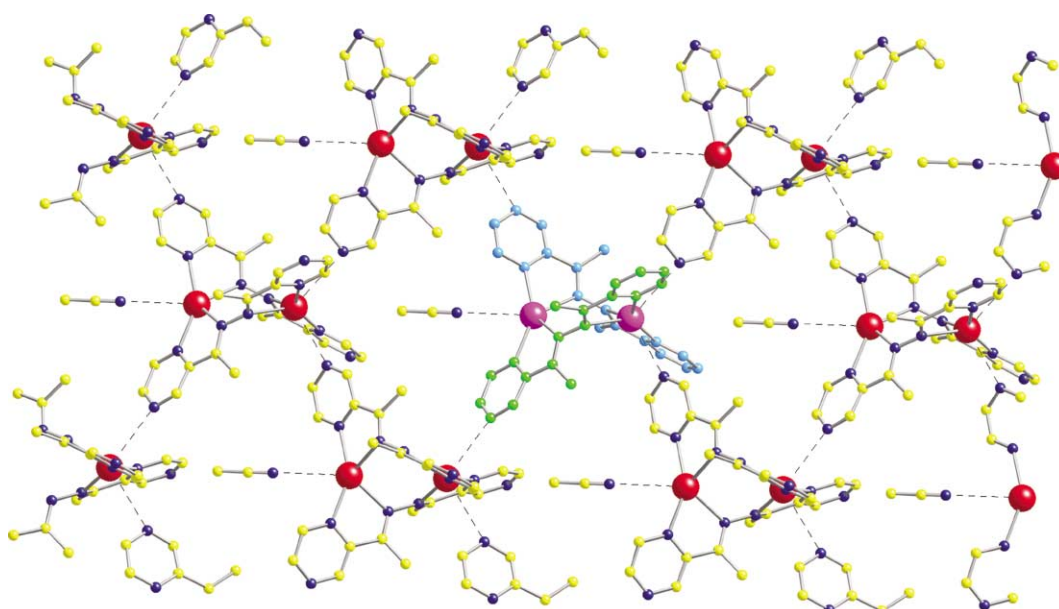


Fig. 4 Structure of the planes of inter-connected double-helical cations in the crystal structure of complex $\{[Ag_2(L_a)_2][PF_6]_2 \cdot MeCN\}_n$. The central cation has been shaded to emphasise the double-helical architecture. Hydrogens are omitted for clarity.

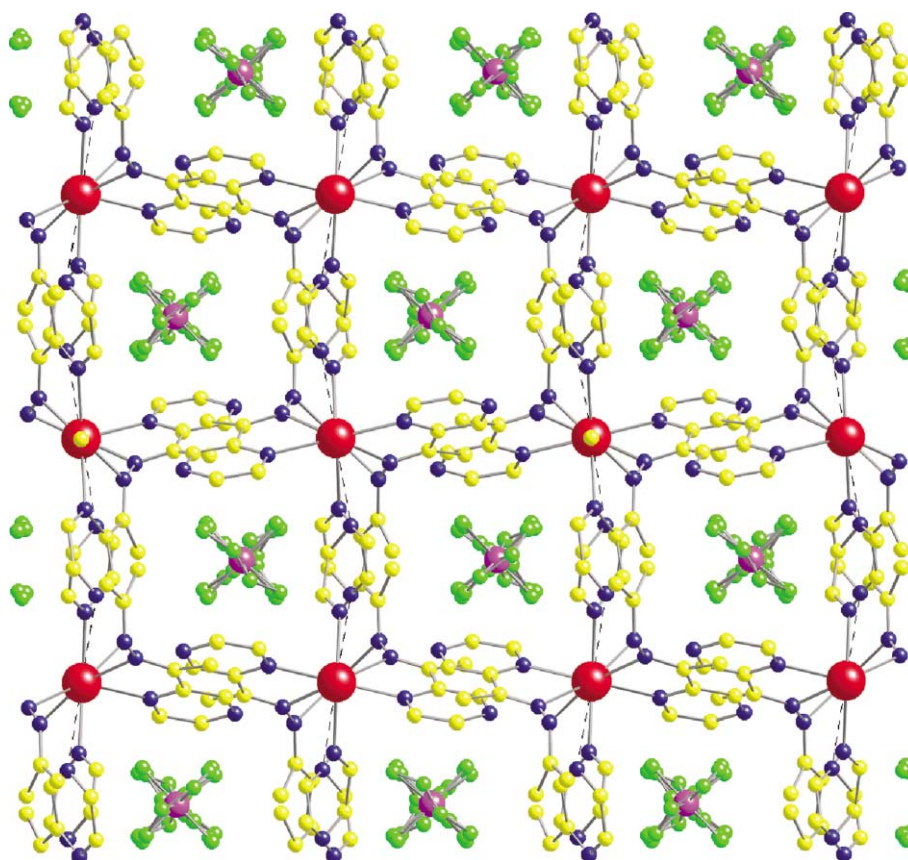


Fig. 5 Packing of the cation layers (which run vertically) and the resulting channels filled with hexafluorophosphate anions in the complex $\{[Ag_2(L_a)_2][PF_6] \cdot MeCN\}_n$. Hydrogens are omitted for clarity.

either with a single solution species or with multiple species interconverting rapidly on the NMR timescale as observed in the corresponding pyridylimine complex.^{7–9} At lower temperature (248 K in CD_3NO_2 and 238 K in CD_3CN) the peaks remained sharp but in nitromethane some small additional peaks were observed in the baseline. The FAB mass spectrum shows Ag_2L_2 peaks, however, we could observe no complex peaks in electrospray (possibly consistent with polymeric solution species). It is therefore unclear whether in solution the complex consists of dinuclear-double helicates or rather (as for the pyridylimine complex) a rapidly interconverting library

comprising a double-helical dimer, with circular helical trimers and possibly tetramers.

The formation of a library of architectures would seem more likely from the pyridylimine chemistry and further support for this comes from a recent paper from Dong and co-workers (which appeared during the preparation of this publication).²⁰ The focus of that paper is the design of crystalline organic–inorganic hybrid networks and describes “the first example of an extended . . . 3D network containing . . . organic, organic/inorganic hybrid and inorganic components”. The paper describes two additional silver(i) complex salts of ligand L_a

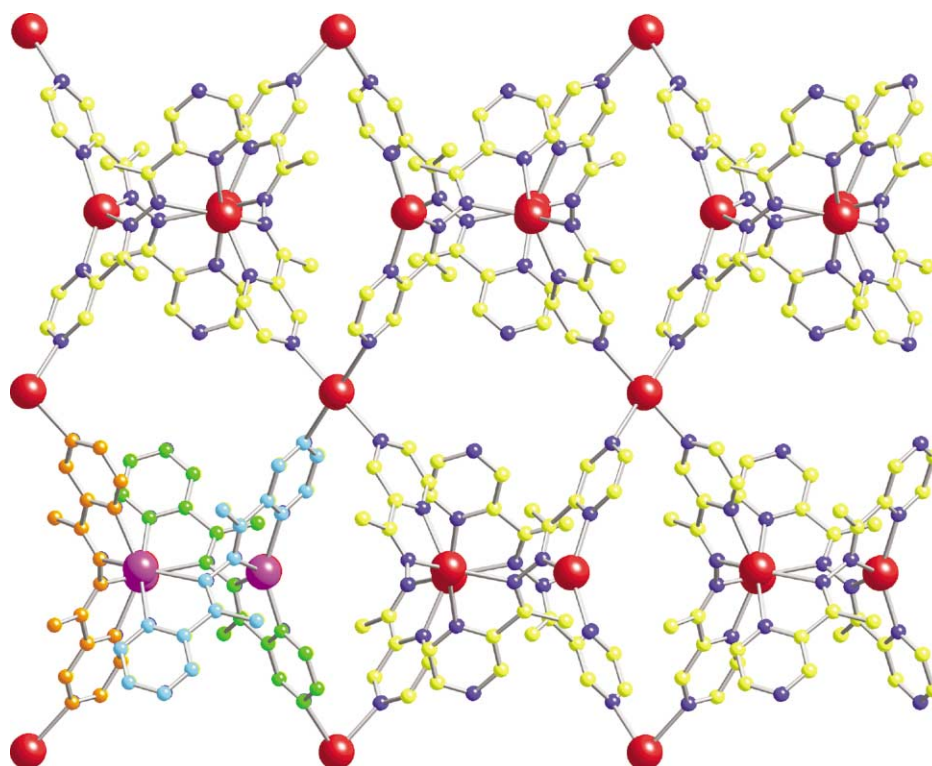


Fig. 6 View illustrating that the cationic network in $\{[Ag_5(L_a)_3(NO_3)_3][Ag(NO_3)_2] \cdot 3CHCl_3\}_n$ reported in ref. 18 represents an aggregated analogue of the trimeric circular helicate that we have previously reported in ref. 8. The strands of the circular helicate in the bottom left corner of the diagram have been coloured to highlight the circular helical nature of the components. Coordinated nitrates, anions, encapsulated solvent and hydrogens have been omitted for clarity.

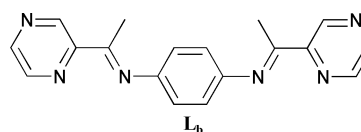
with different anions. Although the focus of that paper lies elsewhere, the structures are clearly pertinent to the design approach that we are exploring. Consequently we have examined these structures in greater detail to explore whether they are also aggregates of the specific architectures that we have characterised for the pyridylimine ligands.

Our analysis of the cationic network in Dong's structure $\{[Ag_5(L_a)_3(NO_3)_3][Ag(NO_3)_2] \cdot 3CHCl_3\}_n$ reveals that it represents an aggregated analogue of the trimeric circular helicate that we have proposed as a component of the solution library for the silver(i) complex of the pyridylimine ligand⁷ and which we have structurally characterised for the corresponding copper(i) complex.⁸ This is illustrated in Fig. 6. The trinuclear circular helicate is formed from three ligands wrapping around three silver(i) centres, affording pseudo-tetrahedral coordination at each silver(i) centre. The circular helical architectures themselves are very similar to the cuprous analogue⁸ that we have previously described. In this silver(i) structure, chloroform solvent molecules are encapsulated into the cavities formed by the aromatic rings on the upper and lower faces of the circular helicate, just as hexafluorophosphate anions and diethyl ether solvent are located in these cavities in the corresponding copper(i) pyridylimine trinuclear circular helicate.⁸ The coordination environment in the trinuclear circular helicate structure does not afford the additional coordination sites (filled with anions or solvent) present in the dinuclear double-helical structures. With such sites not available for aggregation, the nature of the aggregation is consequently different. Rather than the external nitrogens of one unit coordinating to the silver centre of another unit, the monodentate pyrazine donors which point out from these trinuclear units bind to additional silver(i) centres and silver(i) nitrate units which form four and two links, respectively, and link the circular helicates into a 3D array.

Our analysis of the cationic network in Dong's second structure $\{[Ag_2(L_a)_2][SbF_6]_2 \cdot CH_2Cl_2\}_n$ reveals that it represents an aggregate of double-helical architectures. This is illustrated in Fig. 7. In so far as it is an aggregate of double-helices, it is

superficially similar to the structure of the hexafluorophosphate salt that we report herein. Indeed the helical units are again aggregated through coordination of the external nitrogens of one unit to the silver(i) centres of another unit. However, the connectivity of the helicate units is different and this leads to a quite different macromolecular structure. In the PF_6 salt we have described herein, two pyrazines at the *same* end of the helix form connection points and coordinate to the silver(i) centres of adjacent helicates. By contrast, in Dong's SbF_6 structure two pyrazines at *opposite* ends of the helix form connection points. Each silver(i) centre is five-coordinate, bound to a single monodentate pyrazine, and the bond to the monodentate pyrazine (~ 2.6 Å) is consequently shorter than that in our hexafluorophosphate salt.

Silver(i) complex of ligand L_b



To explore the approach further, we investigated the ligand system in which a phenylene unit separates the binding domains (L_b). Reaction of silver(i) with the corresponding bis-pyridylimine ligand²¹ can, depending on the anion, give rise either to tetranuclear grid structures (similar to those reported by Youinou *et al.*²² and by Lehn and co-workers²³) or, more frequently, linear polymers analogous to those we have described with a 1,5-naphthyl spacer.¹⁰ In these structures, the silver(i) centres are bound to two pyridylimine units. However (in contrast to the double-helical structures described for L_a and its pyridylimine analogue⁷⁻⁹) the silver environment is close to tetrahedral and does not have open sites to which additional donors might coordinate. We anticipated that, for L_b , the didentate pyrazylketimine sites should give rise to similar structures to those observed with the corresponding pyridylimine ligand but that the monodentate pyrazyl nitrogens located on the

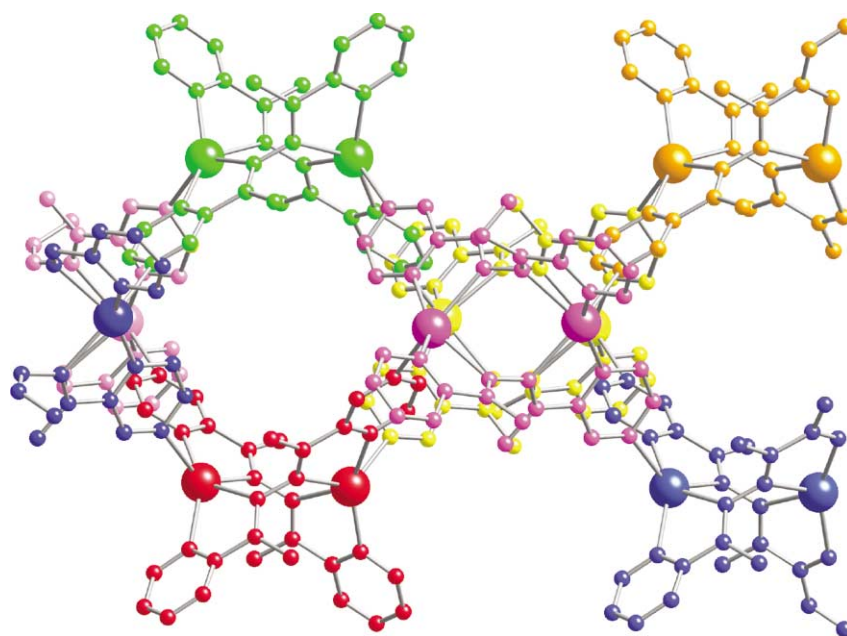


Fig. 7 View illustrating that the cationic network in the structure $\{[Ag_2(L_a)_2][SbF_6]_2 \cdot CH_2Cl_2\}_n$ reported in ref. 18 represents an aggregate of double-helical units. Each double-helicate has been coloured to highlight the nature of the components. Anions, solvent and hydrogens have been omitted for clarity.

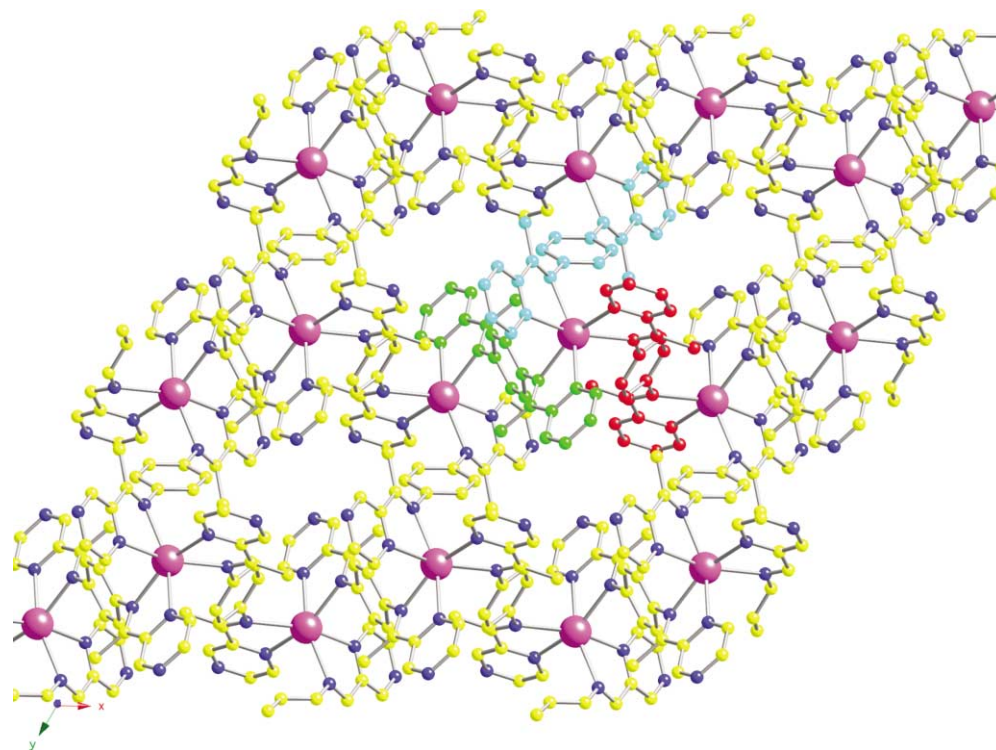


Fig. 8 View of the complex $\{[Ag(L_b)][BF_4]\}_n$ illustrating the brickwork-like network associated with the first type of silver(I) centre. Hydrogens, anions and the second silver(I) sites are omitted for clarity. The three ligands about one silver(I) centre are shaded to illustrate the coordination and connectivity.

exterior would form additional coordinate interactions to other distinct metal centres (rather than to vacant sites on metals supporting the architectural motifs) as seen for the trinuclear circular helicate complex of L_a . Although this is indeed the basic principle of what is observed the lower donor ability of the pyrazine (compared to pyridine) itself introduces further elements of complexity.

Reaction of the ligand L_b with silver(I) acetate followed by precipitation as the tetrafluoroborate anion and recrystallisation from acetonitrile by the slow diffusion of diethyl ether afforded crystals suitable for X-ray characterisation. The structure reveals a complex of 1 : 1 stoichiometry containing two distinct silver(I) centres, one coordinated only to didentate

pyrazylketimine units and the other only to monodentate pyrazine donors. Dealing with each silver(I) centre in turn: The first silver(I) centre is coordinated to three didentate pyrazylketimine units. With pyridylimines the usual coordination number is four and this higher coordination number (six) reflects the lower donor ability of pyrazine. This is also reflected in the $Ag-N_{pz}$ bond lengths of $\sim 2.5 \text{ \AA}$ which are about 10% longer than those to pyridine in pyridylimine complexes. The increase in number of ligands coordinated to the metal leads to a two-dimensional polymeric network with a brickwork-like net structure (rather than a one-dimensional chain observed with the pyridylimines^{10,21}). This is shown in Fig. 8.

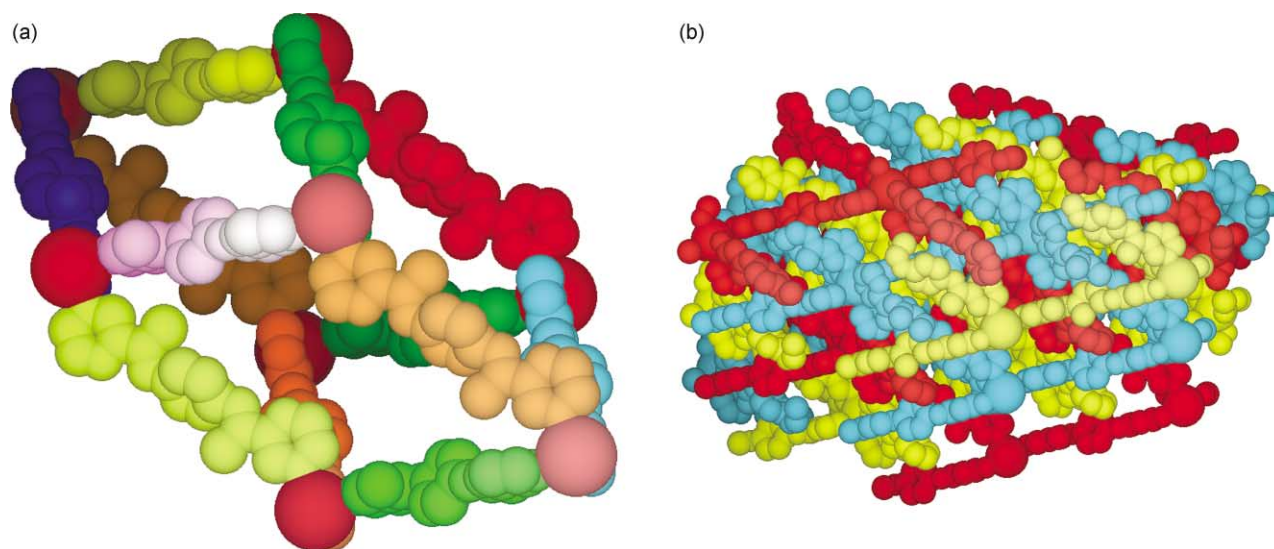


Fig. 9 Space filling views of the complex $\{[Ag(L_b)](BF_4)\}_n$ illustrating the networks associated with the second type of silver(I) centre. Hydrogens, anions and the first silver(I) sites are omitted for clarity. (a) illustrating the rhombohedral cubic nature with different ligands shaded in different colours; (b) illustrating the triple interpenetration of the rhombohedral cubic networks with the three nets shaded in different colours

The second silver(I) centre also has coordination number six and is bound to six monodentate pyrazines. The consequence of this is the formation of a three-dimensional network of cube-like architecture (Fig. 9). Although the angles at the metal are very close to 90° , the monodentate pyrazine donors are not located along the long axis of the ligand but instead located on the rings in a position *ortho* to this axis. Consequently the sides are not located perpendicular at the corners of the cube and thus a network based on rhombohedral cubes results.

For the d^{10} monocations silver(I) and copper(I) coordination numbers of two and four are more usual, and in consequence with bis-monodentate ligands adamantoid networks (coordination number four) or linear chains (coordination number two) are more common. However a variety of different networks have been observed for pyrazine with silver(I)^{15–17} and among these is one example of a cubic network containing six-coordinate silver centres.¹⁵ Despite the great number of metallo-organic coordination frameworks that have been prepared by crystal engineers, three-dimensional cubic metallo-organic coordination networks remain rare. This is somewhat surprising since a cubic network is the logical consequence of interacting all six sites of an octahedral metal centre with a linear bis-monodentate ligand such as 4,4'-bipyridine; Within metallo-organic networks formed by octahedral centres, anions and/or solvent molecules frequently coordinate to the metal, thereby lowering the extent of network connectivity.²⁴ Rectangular-cube shaped hetero-ligand frameworks have been prepared by linking two-dimensional square grids either through coordination or other non-covalent interactions.²⁵

Within three-dimensional network structures, network interpenetration is common, since the voids created by the network are frequently large.²⁶ Indeed the extent of interpenetration is governed by the length of the bis-monodentate ligand. In Ciani's prototypical $\{Ag(pz)_3(SbF_6)\}_n$ cubic metallo-organic framework, the cavities are small and filled by the anions; interpenetration is not observed. In the rhombohedral cuboid network described herein the more extended ligand leads to large voids in the network which are filled by interpenetration of three distinct networks (Fig. 7(b)).

Both types of silver(I) centres (and the networks they give rise to) operate on the same ligands and so the overall structure may be described either:

(i) as planes of two-dimensional brickwork-like net structures separated by planes containing silver(I) centres which bind the monodentate pyrazines from each brickwork-like net (three

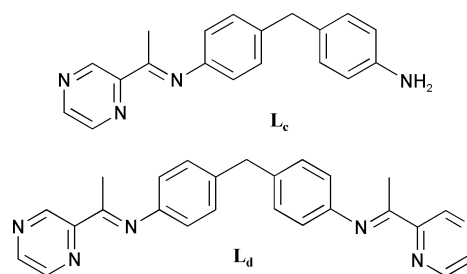
pyrazines per silver from each of two nets) and thereby link the nets together.

(ii) As three interpenetrating rhombohedral cuboid networks which are connected together by silver(I) centres which are each attached to three strands, one from each of the three interpenetrating networks.

The tetrafluoroborate anions reside in small voids in this three-dimensional network and form short contacts to various protons on the ligand strands. Using description (i) of the structure, one anion lies between the brickwork-like nets and forms short contacts to pyrazine and methyl hydrogens, while the other lies within the nets forming short contacts to phenyl and methyl hydrogens. The three pyrazylketimine ligands are oriented in a *fac* conformation and within the two-dimensional brickwork-like nets the chirality at adjacent silver(I) centres alternates, rendering the net achiral. The pyrazylketimine unit is approximately planar (torsion angle 2°) while the phenyl group is twisted through 60° with respect to that plane.

The complex shows poor solubility (consistent with the polymeric structure) except in strongly coordinating solvents such as acetonitrile, in which electrospray MS indicates that the polymeric structure fragments.

Silver(I) complex of ligand L_c



Finally we decided to explore coordination to the ligand system which contains 4,4'-diarylmethane as a spacer (L_d). The bis-pyridyl ketimine analogue of L_d gives dinuclear double-stranded species with either helical (*rac*-) or box (*meso*-) conformation,^{2a,3a} and containing four-coordinate pseudo-tetrahedral silver(I) centres. The ligand structure can support triple-helix formation with metal ions which bind six donors.^{2a} Consequently a series of linked triple-helices (if the silver is six coordinate) or double-stranded structures (if the silver is four coordinate) might be anticipated with L_d .

It did not prove possible to prepare and isolate the ligand L_d directly; a mixture of starting materials and ligands was obtained even on extended reflux with molecular sieves. We have previously encountered similar problems with a bis-pyridylimine ligand containing a binaphthyl spacer, but were able to prepare the complexes directly without isolating the ligand.^{2b} We applied the same approach for this ligand. Solutions of two equivalents of acetylpyrazine and one equivalent of 4,4'-methanedianiline were mixed and heated and then the solution treated with one equivalent of silver(I) tetrafluoroborate to afford a silver(I) tetrafluoroborate salt, crystals of which were obtained from acetonitrile by slow diffusion of tetrahydrofuran. The structure reveals that in this case the silver(I) has found an alternative way to satisfy its coordination requirements; the complex contains not ligand L_d but rather a 'half-ligand' L_c which consists of a pyrazylketimine group at one end with an aniline group at the other. The same initial ligand mixture treated with octahedral metal ions afforded triple-helical complexes of the expected L_d thereby confirming that L_d is available in the solution but has not been selected in this silver(I) complex.²⁷

The structure of this 1 : 1 complex of L_c reveals each ligand to be bridging three silver(I) centres and binding as a didentate pyrazylketimine, a monodentate pyrazine and a monodentate aniline. Each silver(I) centre is bound to three ligands; one as a didentate pyrazylketimine, one as a monodentate pyrazine and the third as a monodentate aniline. The silver(I) centres are five-coordinate with the fifth coordination site being a longer contact to the oxygen of a thf solvent molecule ($Ag \cdots O$ 2.65 Å). The structure consists of planes of networks which extend in two dimensions. Two ligands bridge two metals through the monodentate pyrazine and monodentate aniline groups (Fig. 10) giving a dinuclear double-stranded box-like structure^{2a,3} with the ligands arranged in a head-to-tail configuration.^{3b} This box unit then has two pyrazylketimine units on the outside which link the boxes together to give the polymeric array. Alternatively the structure may be viewed as linear chains formed by coordination through the pyrazylketimine and monodentate pyrazine, and that these chains are linked into a 2D network through coordination to the aniline.

The two-dimensional network sheets are packed together with the thf solvents interdigitated and forming a thf layer separating the coordination planes. The tetrafluoroborate anions are packed towards the edges of the planes by (but not in) the thf layer that separates the planes. They form a number of short contacts to thf, pyrazine, and phenyl hydrogens but the most striking contacts are two hydrogen bonds from the aniline amino hydrogens to two fluorines of the anion ($N-H \cdots F$ 2.09, 2.15 Å; $N-H \cdots F$ 165, 161°; $N \cdots F$ 2.98, 3.03 Å).

As with the other polymeric complexes herein, this complex shows poor solubility in most solvents. Although the complex appears to show some limited solubility in acetonitrile, NMR and electrospray MS indicate that the acetonitrile coordinates to the silver(I) ion causing complex degradation to give a mixture of L_c and starting materials.

Conclusion

The results obtained demonstrate that by introducing pyrazine donor units we can indeed induce higher-order assembly of the supramolecular architectures observed with pyridylimine ligands. Two distinct types of aggregation can occur. In the first, the donors on the outside of one architecture bind to the metals of another architecture to link the units into a polymeric array. In the second type, the donors on the outside of the architectures bind to separate metal centres which are themselves not part of the architectures, and these metals link the units to form the macromolecular array. Both modes are observed in the silver(I) complexes of ligand L_a , with the double-helical units being aggregated by the first mode and the

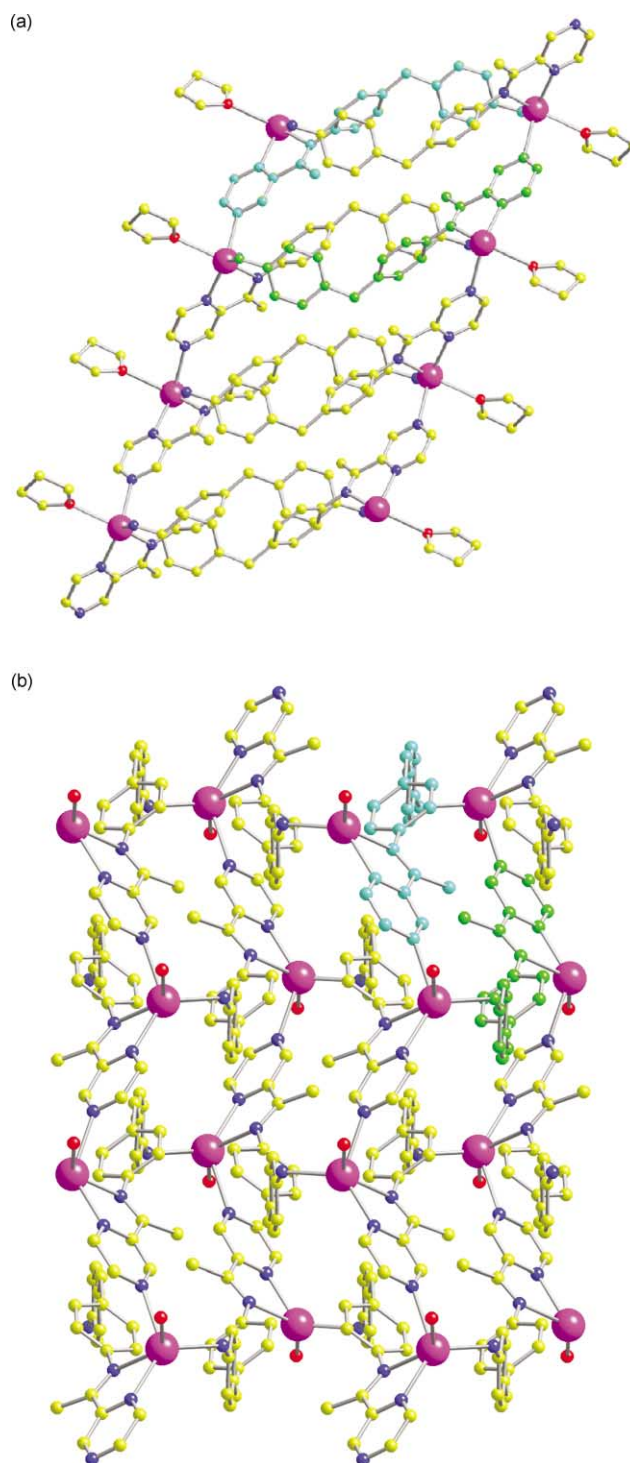


Fig. 10 Views of the complex $\{[Ag(L_c)(thf)][BF_4]\}_n$ illustrating the network. Hydrogens and anions are omitted for clarity: (a) illustrating the planes terminated by the thf layers, with two ligands shaded to illustrate the box structures; (b) the view perpendicular to view (a) and with the carbons of the thf removed for clarity.

trinuclear circular helicates aggregated by the second mode. The second mode is associated with a higher ratio of metal : ligand as observed in the stoichiometry of the complex containing the trinuclear circular helical units. Indeed it seems apparent that in this way (for the L_a ligand system) the metal : ligand stoichiometry can affect which architecture (double-helix or trinuclear circular helix) is selected from the available library of architectures as the building unit for the macromolecular array. For the two double-helical complexes of L_a the connectivity of the helicate units is different and this leads to quite different macromolecular structures. In these two structures not only are the anions different but the solvents from which the salts were

crystallised also differ. In particular, it is striking that in the hexafluorophosphate salt, the silver(I) centre at one end of the helix is coordinated to an acetonitrile solvent molecule and is not involved in the aggregation. By way of contrast, the hexafluoroantimonate salt was crystallised from (and contains) the non-coordinating solvent dichloromethane. Consequently the silver(I) centres at both ends of the helix are available for and engage in the aggregation. Coordinating solvents may therefore be able to play a significant role in determining the aggregation pattern.

Within crystal-engineered coordination polymers, anion effects are common when the anion is coordinated to the metal centre.²⁸ Effects of non-coordinating anions, while less common, can result in switching between different coordination polymer motifs.²⁹ Such anion effects relate both to the ability of the anions to form C–H...X contacts (the number, spatial distribution and nature of their hydrogen bond acceptors) and to the sizes of the anions in relation to the voids in the structures. However, with current knowledge, prediction of potential structures and of how they might be selected by a given anion (or solvent) is not yet feasible. For such a system, guidelines for architecture control are most likely to arise through experimental observation. In this instance, both of the observed macromolecular structures assembled from double-helical units afford tube-like channels in which the anions reside, with the number and pattern of the F...H contacts being similar in both cases.

While the pyrazines do lead to the desired aggregation being achieved, the weaker donor nature of the pyrazine nitrogens (compared to pyridine) introduces an additional element into the design, since higher coordination numbers are favoured. For the two double-helical complexes of **L_a** this feature reinforces the design, providing the increase in coordination sites required to link the units directly without further metal centres. However, since the nature of the discrete architecture is determined by the metal–ligand interactions, the nature of the architecture can also be affected by the switch to pyrazine. This is the case for the **L_b** ligand system in which the expansion in the coordination number (to six) leads to an increase in the connectivity of the array and the formation of a 2D brickwork-like net rather than a 1D linear chain as seen in the corresponding pyridylimine system. The pyrazine nitrogens on the outside of this brickwork-like 2D-net structure are then connected to separate metal centres which link the units to form the macromolecular array, giving aggregation through the second mode. This structure shows further similarities to the aggregate of trinuclear circular helices in that both contain the pyridylimine-type architectural motif (albeit with increased connectivity in the case of **L_b**) linked by planes of connecting silver(I) centres. While the trinuclear circular helical **L_a** structure represents an aggregate of a discrete architecture, the **L_b** structure is in effect an aggregate of a metallo-supramolecular coordination polymer.

The observation of the half-ligand **L_c** complex was unexpected and might be ascribed to the lower donor ability of pyrazine being offset by conversion of one end of the ligand to an amine donor, although the instability of the ligand itself (and of the complex in acetonitrile) implies that the situation may be more complex.

When comparing the metallo-aggregation investigated herein with the H-bond and π – π aggregation approaches that we have previously investigated, it is clear that the design of aggregates is conceptually simpler when two different types of interactions are used in concert (one type for the assembly of the architectures and another for the aggregation)^{5,6} or when the external aggregation site is removed from the architecture assembly site.¹¹ However, the effect of electronically linking the aggregation and architecture assembly sites as in the design herein does also have potential benefits by allowing construction (and subsequent aggregation) of architectures not

normally accessible with the pyridylimines, as illustrated for **L_b**. This is the subject of continuing studies in our laboratories.

Experimental

General

All starting materials were purchased from Aldrich and used without further purification. Infrared spectra were recorded with a Perkin Elmer Paragon 1000 FTIR spectrometer from KBr pellets. NMR spectra were recorded on Brüker DPX 300 and 400 instruments using standard Brüker software. FAB mass spectra were recorded by the Warwick mass spectrometry service on a Micromass Autospec spectrometer using 3-nitrobenzyl alcohol as matrix. Electrospray ionisation (ESI) analyses were performed by the EPSRC National Mass Spectrometry Service Centre, Swansea on a Micromass Quatro (II) in positive ionisation mode. Samples were loop injected into a stream of water–methanol (1 : 1). Nebulisation was pneumatically assisted by a flow of nitrogen through a sheath around the capillary. Capillary (ionising) voltage + 3.5 kV; source voltage 20 V. Microanalyses were conducted on a Leeman Labs CE44 CHN analyser by the University of Warwick Analytical Service.

Syntheses

Preparation of **L_a.** To a stirred solution of acetylpyrazine (0.244 g, 2 mmol) in methanol was added dropwise hydrazine monohydrate (0.05 g, 1 mmol) and a few drops of glacial acetic acid. The mixture was heated under reflux for 4 h and then cooled to room temperature. Orange crystals precipitated from the solution on standing and were collected by vacuum filtration and washed with methanol (0.2 g, 83%). X-Ray quality, orange crystals were obtained by slow evaporation of the solution.

Mass spectrum (FAB): m/z 241 [M + H]⁺.

Elemental analysis: calc. (%) for C₁₂H₁₂N₆: C: 59.9, H: 5.0, N: 34.9; found: C: 59.8, H: 5.0, N: 34.8.

¹H NMR (300 MHz, CDCl₃, 298 K): δ 9.46 (1H, s, H³), 8.58 (2H, m, H⁵, H⁶), 2.37 (3H, s, CH₃).

IR: ν 3047 (m), 1611 (m), 1571 (m), 1466 (s), 1397 (m), 1363 (vs), 1301 (m), 1158 (m), 1101 (m), 1046 (m), 1012 (vs), 849 (s), 757 (w), 653 (m) cm⁻¹.

Coordination of **L_a to silver(I).** Care was taken to exclude light during the following procedure: Ligand **L_a** (0.024 g, 0.1 mmol) and silver(I) hexafluorophosphate (0.025 g, 0.1 mmol) were stirred in methanol for 30 min. The resulting yellow precipitate (0.074 g, 75%) was collected by vacuum filtration and washed with methanol. X-Ray quality, pale yellow crystals were obtained by slow diffusion of tetrahydrofuran into a solution of the complex in acetonitrile.

Mass spectrum (FAB) m/z 841 [Ag₂L₂(PF₆)], 696 [Ag₂L₂].

Elemental analysis: calc. (%) for [Ag₂(C₁₂H₁₂N₆)₂](PF₆)₂·H₂O: C: 28.7, H: 2.6, N: 16.7; found: C: 28.9, H: 2.6, N: 16.6.

¹H NMR (400 MHz, CD₃NO₂, 298 K): δ 9.11 (1H s, H³), 8.85 (1H d, J = 2.5 Hz, H^{5/6}), 8.69 (1H, dd, J = 2.5, 1.5 Hz, H^{5/6}), 2.29 (3H, s, CH₃).

IR: ν 3647 (w), 1614 (m), 1571 (m), 1405 (m), 1371 (m), 1319 (s), 1163 (m), 1128 (m), 1051 (s), 1034 (m), 831 (vs), 736 (w), cm⁻¹.

Preparation of **L_b.** To a stirred solution of acetylpyrazine (0.244 g, 2 mmol) in methanol was added dropwise 1,4-phenylenediamine in methanol (0.104 g, 1 mmol) and a few drops of glacial acetic acid. The mixture was heated under reflux for 3 h and then cooled to room temperature. A yellow solid precipitated from the solution on standing and was collected by filtration and washed with methanol (0.268 g, 85%).

Mass spectrum (FAB): m/z 317 [M + H]⁺.

Table 1 Crystallographic data and details of refinement

	L_a	$\{[Ag_2(L_a)_2][PF_6]_2 \cdot MeCN\}_n$	$\{[Ag(L_b)][BF_4]\}_n$	$\{[Ag(L_c)][BF_4] \cdot thf\}_n$
Empirical formula	$C_{12}H_{12}N_6$	$C_{26}H_{27}Ag_2F_{12}N_{13}P_2$	$C_{18}H_{16}AgBF_4N_6$	$C_{23}H_{26}AgBF_4N_4O$
M_r	240.28	1027.29	511.05	569.16
T/K	180(2)	180(2)	180(2)	180(2)
Crystal system	Monoclinic	Orthorhombic	Trigonal	Monoclinic
Space group	$P2_1/n$	$Pbcn$	$P\bar{3}$	$P2_1/c$
$a/\text{\AA}$	4.4272(16)	15.1092(4)	10.3804(11)	18.4389(13)
$b/\text{\AA}$	7.440(3)	15.3225(4)	10.3804(11)	9.8630(6)
$c/\text{\AA}$	17.810(6)	15.7434(12)	16.099(3)	13.5869(9)
$\beta/^\circ$	90.344(9)	90	90	106.578(2)
$U/\text{\AA}^3$	586.6(4)	3644.8(3)	1502.3(3)	2368.2(3)
Z	2	4	3	4
$D/g\text{ cm}^{-3}$	1.360	1.872	1.695	1.596
μ/mm^{-1}	0.090	1.265	1.060	0.906
Reflections collected	3516	17193	7601	11833
Independent reflections (R_{int})	1411 (0.0402)	4507 (0.0492)	1780 (0.1133)	4151 (0.1737)
Parameters	83	292	164	326
Goodness-of-fit on F^2	0.877	0.812	1.003	0.987
Final R indices [$I > 2\sigma(I)$]	$R_1 = 0.0497$, $wR_2 = 0.1236$	$R_1 = 0.0357$, $wR_2 = 0.0933$	$R_1 = 0.0561$, $wR_2 = 0.1048$	$R_1 = 0.0700$, $wR_2 = 0.1430$

Elemental analysis: calc. (%) for $C_{18}H_{16}N_6$: C: 68.3, H: 5.1, N: 26.6; found: C: 68.2, H: 5.1, N: 26.5

1H NMR (300 MHz, CD_2Cl_2 , 298 K): δ 9.49 (2H, s, H^3), 8.63 (2H, m, H^5 , H^6), 6.93 (4H, s, H^{Ph}), 2.42 (6H, s, CH_3).

IR: ν 2989 (w), 1635 (s), 1571 (w), 1519 (w), 1494 (s), 1470 (m), 1404 (s), 1362 (s), 1298 (m), 1228 (m), 1153 (m), 1100 (s), 1044 (s), 1014 (s), 969 (w), 850 (vs), 749 (m), cm^{-1} .

Coordination of L_b to silver(I). Care was taken to exclude light during the following procedure: Ligand L_b (0.054 g, 0.17 mmol) and silver(I) acetate (0.028 g, 0.17 mmol) in methanol were heated under reflux for 30 min, cooled to room temperature, filtered through Celite and treated with methanolic ammonium tetrafluoroborate. The resulting orange precipitate was collected by vacuum filtration and washed with methanol (0.056 g, 64%). X-Ray quality, pale orange crystals were obtained by slow diffusion of diethyl ether into a solution of the complex in acetonitrile.

Mass spectrum (FAB): m/z 425 $[AgL]^+$.

Mass spectrum (ES; MeCN) m/z 425 $[AgL]^+$, 317 $[LH]^+$.

Elemental analysis: calc. (%) for $[Ag(C_{18}H_{16}N_6)(BF_4) \cdot H_2O]_n$: C: 40.9, H: 3.5, N: 15.9; found: C: 41.0, H: 3.1, N: 15.9

1H NMR (400 MHz, CD_3CN , 298 K): δ 9.39 (1H s, H^3), 8.73 (1H d, $J = 2.5$ Hz, $H^{5/6}$), 8.65 (1H, dd, $J = 1.5, 0.75$ Hz, $H^{5/6}$), 6.95 (2H, s, H^{Ph}), 2.40 (3H, s, CH_3).

IR: ν 2996 (w), 1632 (m), 1448 (m), 1401 (m), 1373 (m), 1304 (m), 1220 (m), 1173 (w), 1122 (m), 1045 (vs), 858 (m), 749 (w), cm^{-1} .

Preparation of L_c and coordination to silver(I). To a stirred solution of acetylpyrazine (0.041 g, 0.30 mmol) and ground 3Å dried molecular sieves in methanol was added dropwise bis-(4-aminophenyl)methane (0.033 g, 0.15 mmol) in methanol and a few drops of glacial acetic acid. The mixture was heated under reflux for 24 h. The molecular sieves were removed by filtration and the filtrate treated with silver(I) tetrafluoroborate (0.029 g, 0.15 mmol) and stirred for 30 min. The resulting yellow precipitate (0.051 g, 68%) was collected by vacuum filtration and washed with methanol. X-Ray quality, pale yellow crystals were obtained by slow diffusion of tetrahydrofuran into a solution of the complex in acetonitrile.

Mass spectrum (FAB): m/z 411 $[AgL]^+$.

Elemental analysis: calc. (%) for $[Ag(C_{19}H_{18}N_4)(BF_4) \cdot 0.5MeOH]_n$: C: 45.6, H: 3.9, N: 10.9; found: C: 46.1, H: 3.9, N: 10.6

IR: ν 3305 (w), 1612 (m), 1512 (s), 1440 (m), 1409 (m), 1372 (m), 1313 (m), 1224 (m), 1178 (m), 1128 (m), 1051 (vs), 831 (m), 764 (w), cm^{-1} .

X-Ray crystallography

Crystallographic data are collected in Table 1. Crystal data for the compounds were collected with a Siemens-SMART-CCD diffractometer³⁰ equipped with an Oxford Cryosystem Cryostream Cooler.³¹ Refinements used SHELXTL.³² Systematic absences indicated the appropriate space groups, shown to be correct by successful refinements. The structures were solved by direct methods with additional light atoms found by Fourier methods. Hydrogen atoms were added at calculated positions and refined using a riding model with freely rotating methyl groups. Anisotropic displacement parameters were used for all non-H atoms; H-atoms were given isotropic displacement parameters equal to 1.2 (or 1.5 for methyl hydrogen atoms) times the equivalent isotropic displacement parameter of the atom to which the H-atom is attached.

CCDC reference numbers 233558–233561.

See <http://www.rsc.org/suppdata/dt/b4/b403749a/> for crystallographic data in CIF or other electronic format.

$\{[Ag_2(L_a)_2][PF_6]_2 \cdot MeCN\}_n$. The asymmetric unit contains one ligand and two half silvers, a disordered PF_6 and half an acetonitrile solvent molecule. The PF_6 is disordered about the equator over two positions with nearly equal occupancy. The acetonitrile lies on special position (4c) as do both silver ions.

$\{[Ag(L_b)][BF_4]\}_n$. The asymmetric unit contains half a ligand with two silvers and two BF_4 groups on special positions. Ag1 lies on the three-fold inversion axis, and Ag2 lies on a three-fold axis. B10 lies on a three-fold axis and B20 lies on three-fold axis. F21 lies on the three-fold inversion axis and the B20 BF_4 is disordered in two positions about F21 along the three-fold axis. The B10 BF_4 was very disordered and the fluorines were modelled over two positions (occupancy 7 : 3) with one of the fluorines of the minor component (F14) lying on the three-fold axis (position 3d).

$\{[Ag(L_c)][BF_4] \cdot thf\}_n$. The asymmetric unit contains a mono pyridine imine ligand with a free amine end, a silver, a disordered BF_4 and a disordered THF. The THF disorder was modelled as two related envelope forms that share the some O001 C003 and C004. These were fixed at 50 : 50 occupancy. The fluorines of the BF_4 were disordered over two positions (occupancy 9 : 1) with the minor component refined isotropically.

L_a . The asymmetric unit contains half a molecule as the molecule lies on an inversion centre between the two nitrogens of the aza group.

Acknowledgements

This work was supported by an EU Marie Curie Individual Fellowship (F. T.; MCFI-2000-00403) and EU Marie Curie Training Site Fellowships in Supramolecular and Macromolecular Chemistry (M. P.; HPMT-GH-01-00365-11; G. I. P.; HPMT-GH-01-00365-10; E. J. K.; HPMT-GH-01-00365-14). We thank EPSRC and Siemens Analytical Instruments for grants in support of the diffractometer and the EPSRC National Mass Spectrometry Service Centre, Swansea for recording the electrospray mass spectra.

References

- D. Philp and J. F. Stoddart, *Angew. Chem., Int. Ed.*, 1996, **35**, 1154; J.-M. Lehn, *Supramolecular Chemistry – Concepts and Perspectives*, VCH, Weinheim, 1995; *Comprehensive Supramolecular Chemistry*, ed. J. L. Atwood, J. E. D. Davies, J.-M. Lehn, D. D. MacNicol and F. Vogtle, Pergamon, Oxford, 1996; C. Piguet, G. Bernardinelli and G. Hopfgartner, *Chem. Rev.*, 1997, **97**, 2005; M. Albrecht, *J. Inclusion Phenom., Macrocycl. Chem.*, 2000, **36**, 127; A. F. Williams, *Pure Appl. Chem.*, 1996, **68**, 1285; C. Dietrich-Buchecker, G. Rapenne and J. P. Sauvage, *Coord. Chem. Rev.*, 1999, **186**, 167; M. Fujita, *Acc. Chem. Res.*, 1999, **32**, 53; B. Olenyuk, A. Fechtenkötter and P. J. Stang, *J. Chem. Soc., Dalton Trans.*, 1998, 1707; D. L. Caulder and K. N. Raymond, *Acc. Chem. Res.*, 1999, **32**, 975; D. W. Johnson and K. N. Raymond, *Supramol. Chem.*, 2001, **13**, 637; E. C. Constable, *Prog. Inorg. Chem.*, 1994, **42**, 67; R. W. Saalfrank and I. Bernt, *Curr. Opin. Solid State Mater. Sci.*, 1998, **3**, 407; M. Albrecht, *Chem. Rev.*, 2001, **101**, 3457; L. J. Childs and M. J. Hannon, *Supramol. Chem.*, 2004, **16**, 7.
- (a) M. J. Hannon, C. L. Painting, J. Hamblin, A. Jackson and W. Errington, *Chem. Commun.*, 1997, 1807; (b) J. Hamblin, L. J. Childs, N. W. Alcock and M. J. Hannon, *J. Chem. Soc., Dalton Trans.*, 2002, 164; (c) M. J. Hannon, I. Meistermann, C. J. Isaac, C. Blomme, J. R. Aldrich-Wright and A. Rodger, *Chem. Commun.*, 2001, 1078; (d) A. Lavalette, J. Hamblin, A. Marsh, D. M. Haddleton and M. J. Hannon, *Chem. Commun.*, 2002, 3040.
- (a) M. J. Hannon, C. L. Painting and N. W. Alcock, *Chem. Commun.*, 1999, 2023; (b) M. J. Hannon, S. Bunce, A. J. Clarke and N. W. Alcock, *Angew. Chem., Int. Ed.*, 1999, **38**, 1277.
- I. Meistermann, V. Moreno, M. J. Prieto, E. Moldrheim, E. Sletten, S. Khalid, P. M. Rodger, J. C. Peberdy, C. J. Isaac, A. Rodger and M. J. Hannon, *Proc. Natl. Acad. Sci. USA.*, 2002, **99**, 5069; M. J. Hannon, V. Moreno, M. J. Prieto, E. Molderheim, E. Sletten, I. Meistermann, C. J. Isaac, K. J. Sanders and A. Rodger, *Angew. Chem., Int. Ed.*, 2001, **40**, 879; E. Molderheim, I. Meistermann, A. Rodger, M. J. Hannon and E. Sletten, *J. Biol. Inorg. Chem.*, 2002, **7**, 770; M. J. Hannon and A. Rodger, *Pharm. Visions*, 2002, Autumn issue, p. 14.
- L. J. Childs, N. W. Alcock and M. J. Hannon, *Angew. Chem., Int. Ed.*, 2002, **41**, 4244; L. J. Childs, N. W. Alcock and M. J. Hannon, *Angew. Chem., Int. Ed.*, 2001, **40**, 1079.
- A. Lavalette, F. Tuna, G. Clarkson, N. W. Alcock and M. J. Hannon, *Chem. Commun.*, 2003, 2666.
- J. Hamblin, A. Jackson, N. W. Alcock and M. J. Hannon, *J. Chem. Soc., Dalton Trans.*, 2002, 1635.
- F. Tuna, J. Hamblin, A. Jackson, G. Clarkson, N. W. Alcock and M. J. Hannon, *Dalton Trans.*, 2003, 2141.
- F. Tuna, G. Clarkson, N. W. Alcock and M. J. Hannon, *Dalton Trans.*, 2003, 2149.
- F. Tuna, J. Hamblin, G. Clarkson, W. Errington, N. W. Alcock and M. J. Hannon, *Chem. Eur. J.*, 2002, **8**, 4957.
- M. J. Hannon, C. L. Painting and W. Errington, *Chem. Commun.*, 1997, 1805.
- N. W. Alcock, P. R. Barker, J. M. Haider, M. J. Hannon, C. L. Painting, Z. Pikramenou, E. A. Plummer, K. Rissanen and P. Saarenketo, *J. Chem. Soc., Dalton Trans.*, 2000, 1447; H. Krass, E. A. Plummer, J. M. Haider, P. R. Barker, N. W. Alcock, Z. Pikramenou, M. J. Hannon and D. G. Kurth, *Angew. Chem., Int. Ed.*, 2001, **40**, 3862.
- See, for example: R. F. Carina, G. Bernardinelli and A. F. Williams, *Angew. Chem., Int. Ed.*, 1993, **32**, 1463; E. Breuning, U. Ziener, J.-M. Lehn, E. Wegelius and K. Rissanen, *Eur. J. Inorg. Chem.*, 2001, 1515; Z. Qin, M. C. Jennings and R. J. Puddephatt, *Chem. Commun.*, 2001, 2676; S.-Y. Yu, T. Kusukawa, K. Biradha and M. Fujita, *J. Am. Chem. Soc.*, 2000, **122**, 2665; R. W. Saalfrank, I. Bernt and F. Hampel, *Chem. Eur. J.*, 2001, **7**, 2770; E. C. Constable, A. J. Edwards, P. R. Raithby and J. V. Walker, *Angew. Chem., Int. Ed.*, 1993, **32**, 1465; M. Vázquez, A. Taglietti, D. Gatteschi, L. Sorace, C. Sangregorio, A. M. González, M. Maneiro, R. M. Pedrido and M. R. Bermejo, *Chem. Commun.*, 2003, 1840.
- For examples of supramolecular helicates aggregated in covalent macromolecular structures, see: A. Lavalette, J. Hamblin, A. Marsh, D. M. Haddleton and M. J. Hannon, *Chem. Commun.*, 2002, 3040; H. Houjou, Y. Shimizu, N. Koshizaki and M. Kanetsato, *Adv. Mater.*, 2003, **15**, 1458.
- L. Carlucci, G. Ciani, D. M. Proserpio and A. Sironi, *Angew. Chem., Int. Ed.*, 1995, **34**, 1895.
- R. G. Vranka and E. L. Amma, *Inorg. Chem.*, 1996, **5**, 1020; L. Carlucci, G. Ciani, D. M. Proserpio and A. Sironi, *J. Am. Chem. Soc.*, 1995, **117**, 4562; L. Carlucci, G. Ciani, D. M. Proserpio and A. Sironi, *Inorg. Chem.*, 1995, **34**, 5698; D. Venkataraman, S. Lee, J. S. Moore, P. Zhang, K. A. Hirsch, G. B. Gardner, A. C. Covey and C. L. Prentice, *Chem. Mater.*, 1996, **8**, 2030; A. J. Blake, N. R. Champness, M. Crew and S. Parsons, *New J. Chem.*, 1999, **23**, 13.
- A. N. Khlobystov, A. J. Blake, N. R. Champness, D. A. Lemenovskii, A. G. Majouga, N. V. Zyk and M. Schröder, *Coord. Chem. Rev.*, 2001, **222**, 155.
- E. C. Kesslen and W. B. Euler, *Chem. Mater.*, 1999, **11**, 336.
- D. Guo, C. He, C. Y. Duan, C. Q. Qian and Q. J. Meng, *New J. Chem.*, 2002, **26**, 796.
- Y.-B. Dong, X. Zhao, B. Tang, H.-Y. Wang, R. Q. Huang, M. D. Smith and H.-C. zur Loye, *Chem. Commun.*, 2004, 220.
- L. J. Childs, PhD Thesis, University of Warwick, UK, 2002; N. Mourtzis, F. Tuna, L. J. Childs, J. Hamblin, D. Yannakopoulou, W. Errington, N. W. Alcock, G. Clarkson and M. J. Hannon, manuscript in preparation.
- M.-T. Youinou, N. Rahmouni, J. Fischer and J. A. Osborn, *Angew. Chem., Int. Ed.*, 1992, **31**, 733.
- P. N. W. Baxter, J.-M. Lehn, J. Fischer and M.-T. Youinou, *Angew. Chem., Int. Ed.*, 1994, **33**, 2284.
- This may reflect at-metal steric crowding associated with heterocycles interacting with the relatively small first row transition metals. First row metals are often preferred for crystal engineering because of the labile nature of the bonds they form, which allows reversible assembly and consequent access to the thermodynamic product.
- See, for example: R. W. Gable, B. F. Hoskins and R. Robson, *J. Chem. Soc., Chem. Commun.*, 1990, 1677; S. Subramanian and M. J. Zaworotko, *Angew. Chem., Int. Ed.*, 1995, **34**, 2117; J. Tao, M.-L. Tong and X.-M. Chen, *J. Chem. Soc., Dalton Trans.*, 2000, 3669; F. A. Almeida Paz, Y. Z. Khimyak, A. D. Bond, J. Rocha and J. Klinowski, *Eur. J. Inorg. Chem.*, 2002, 2823.
- See, for example: A. J. Blake, N. R. Champness, P. Hubberstey, W.-S. Li, M. A. Withersby and M. Schröder, *Coord. Chem. Rev.*, 1999, **183**, 117.
- F. Tuna and M. J. Hannon, unpublished results.
- See, for example: C. V. K. Sharma, S. T. Griffin and R. D. Rogers, *Chem. Commun.*, 1998, 215; M. A. Withersby, A. J. Blake, N. R. Champness, P. Hubberstey, W. S. Li and M. Schröder, *Angew. Chem.*, 1997, **109**, 2421; M. A. Withersby, A. J. Blake, N. R. Champness, P. Hubberstey, W. S. Li and M. Schröder, *Angew. Chem., Int. Ed. Engl.*, 1997, **36**, 2327; S. R. Batten, J. C. Jeffery and M. D. Ward, *Inorg. Chim. Acta*, 1999, **292**, 231; L. R. Hanton and K. Lee, *J. Chem. Soc., Dalton Trans.*, 2000, 1161.
- M. J. Hannon, C. L. Painting, E. A. Plummer, L. J. Childs and N. W. Alcock, *Chem. Eur. J.*, 2002, **8**, 2225; S. Lopez and S. W. Keller, *Inorg. Chem.*, 1999, **38**, 1883; K. A. Hirsch, S. R. Wilson and J. S. Moore, *Inorg. Chem.*, 1997, **36**, 2960.
- SMART user's manual, Siemens Industrial Automation Inc., Madison, WI, 1994.
- J. Cosier and A. M. Glazer, *J. Appl. Crystallogr.*, 1986, **19**, 105.
- G. M. Sheldrick, *Acta Crystallogr., Sect. A*, 1990, **46**, 467.